A study of the solid state `amorphization' reaction in $Fe_{58}Ta_{42}$ by diffraction and Mössbauer spectrometry

1997 J. Phys.: Condens. Matter 9 1425

(http://iopscience.iop.org/0953-8984/9/7/008)

J. Phys.: Condens. Matter **9** (1997) 1425–1433. Printed in the UK PII: S0953-8984(97)75924-1

A study of the solid state 'amorphization' reaction in $Fe_{58}Ta_{42}$ by diffraction and Mössbauer spectrometry

R J Cooper†, N Randrianantoandro‡, N Cowlam†‡ and J-M Greneche‡

† Department of Physics, University of Sheffield, Sheffield S3 7RH, UK

‡ Laboratoire de Physique de l'Etat Condensé, URA CNRS 807, Université du Maine, 72017 Le Mans Cédex, France

Received 3 July 1996, in final form 13 November 1996

Abstract. The solid state 'amorphization' reaction produced by the mechanical alloying (MA) of samples of the eutectic alloy $Fe_{58}Ta_{42}$ has been studied using x-ray and neutron diffraction and ^{57}Fe Mössbauer spectrometry. The consumption of the parent elements as a function of time of MA treatment has been derived from the reduction in intensity of their Bragg peaks in the diffraction patterns. The change of volume fraction of the parent α-iron phase with increasing time of MA treatment has been determined from the reduction in intensity of the sextet in the Mössbauer spectra. The diffraction data and spectrometry data are in good *overall* agreement and both show that the reaction is very rapid in this eutectic alloy and that the parent iron and tantalum powders are transformed into an amorphous phase after only 6 h MA treatment in a conventional Spex 8000 high-energy ball mill. In *detail*, the consumptions of the parent elements derived from the two kinds of measurement are slightly different. This is possibly because the diffraction data represent an average over the whole sample while the Mössbauer spectrometry data are site specific.

1. Introduction

Transition metal–refractory metal (TM–RM) alloys form an interesting class of materials which have the potential for exhibiting useful magnetic properties combined with considerable physical hardness. Alloys of the type including Ni–Ta [1], Fe–W [2], Rh–Ta and Nd–Ir [3], in which the constituents have rather similar atomic sizes are known to glass form over a narrow composition range close to the equiatomic value. However, they have high melting points, which make their molten alloys difficult to contain in conventional quartz crucibles. This problem is not encountered in the preparation of amorphous TM–RM alloys by sputtering [4] or by solid state reactions [5–7]. We have recently begun a systematic investigation of the formation and properties of TM–RM amorphous alloys produced by MA treatments using a Spex 8000 high-energy ball mill, concentrating on studies of the crystalline-to-amorphous transition by diffraction [8] and Mössbauer spectrometry measurements. The preliminary results on the production of eutectic $Fe_{58}Ta_{42}$ amorphous alloys which are presented in this letter, demonstrate that the reaction is very rapid.

2. Sample preparation and experimental methods

Iron and tantalum powders of 3N purity, supplied by Aldrich Chemical Company, were mixed in the atomic concentration $Fe_{58}Ta_{42}$, which corresponds to a high-temperature

0953-8984/97/071425+09$19.50

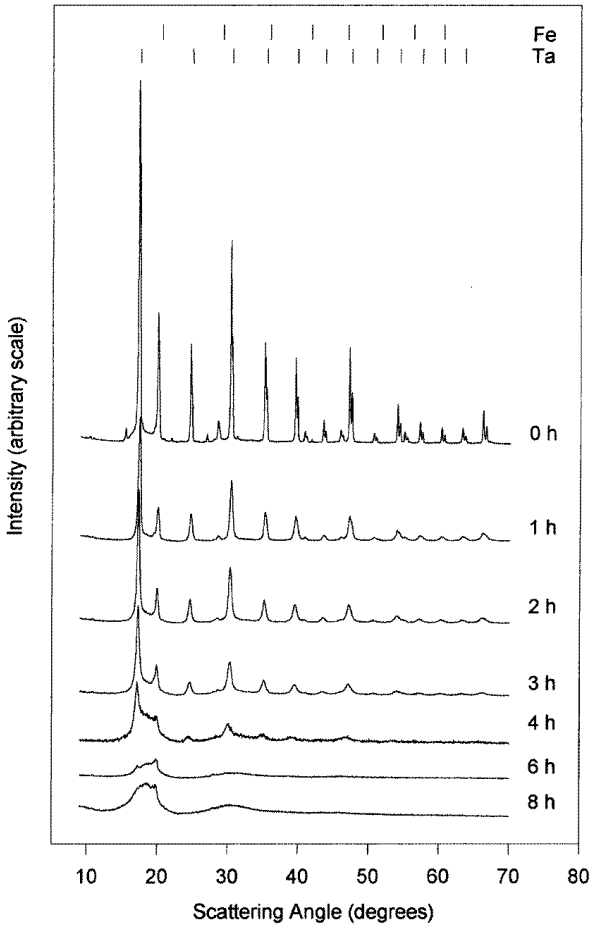

Figure 1. The x-ray diffraction patterns for the $Fe_{58}Ta_{42}$ alloys MA treated for 0 (parent), 1, 2, 3, 4, 6 and 8 h obtained with molybdenum Kα radiation as a function of scattering angle 2θ.

($\approx$1550 °C) eutectic point in the phase diagram. The samples were subjected to MA treatments of 0 (parent), 1, 2, 3, 4, 6, 8, 10, 16 and 24 h using a Spex 8000 mixer–mill, which works with a constant and fixed intensity of milling. A tool steel vial, two 12 mm steel balls and a standard charge of 6 g powder were used and the MA was performed under argon to prevent oxidation. X-ray diffraction experiments were performed using a Philips PW1050 vertical diffractometer with a graphite CCM and molybdenum radiation, $\lambda = 0.711$Å. The samples were measured over scattering angles $7^\circ \leqslant 2\theta \leqslant 70^\circ$. Neutron diffraction measurements were made on the LAD instrument at the ISIS, DRAL, Chilton. The specimens were measured in thin-walled vanadium tubes and background and normalization scans were also performed. The Mössbauer spectrometry measurements were performed in transmission geometry at liquid nitrogen temperature (77 K) using a constant-acceleration-signal spectrometer with a ^{57}Co source diffused into a rhodium matrix. The sample consisted of a mixture of the MA treated powder and BN powder enclosed within a thin capsule 20 mm in diameter.

The x-ray diffraction patterns for a series of the $Fe_{58}Ta_{42}$ samples are shown in figure 1.

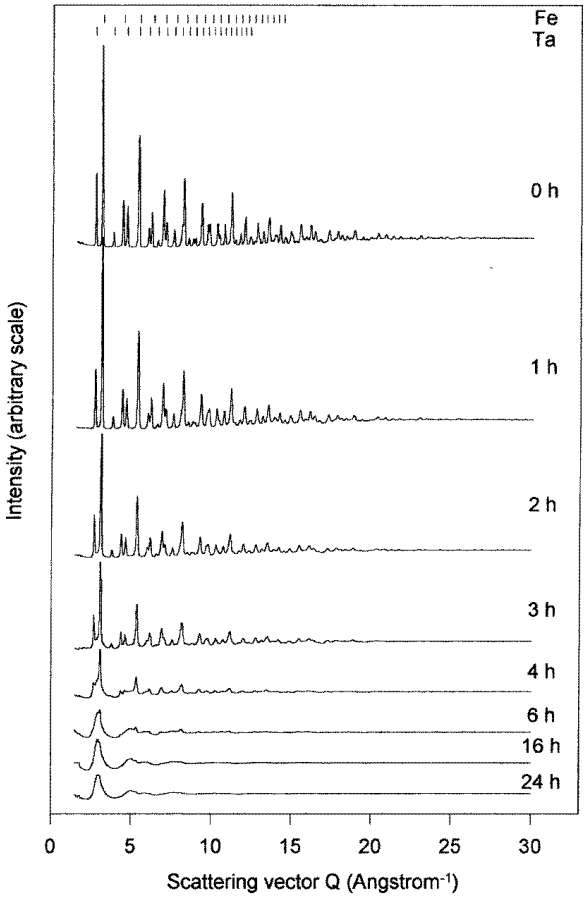

Figure 2. The neutron diffraction patterns for the $Fe_{58}Ta_{42}$ alloys MA treated for 0 (parent), 1, 2, 3, 4, 6, 16 and 24 h obtained with the LAD instrument at the ISIS source as a function of scattering vector Q.

The patterns for the samples with short times of MA treatment exhibit well defined Bragg peaks from the b.c.c. iron and b.c.c. tantalum which are identified at the top of the figure. The visibility of each phase present in the sample is proportional to its total scattering, $N_i\langle\phi_i^2\rangle$, where N_i is the number of atoms in the phase i and $\langle\phi_i\rangle$ is the average scattering amplitude, which is taken to be the atomic scattering factor $f(Q)$ for x-rays (the atomic number Z in the limit of forward scattering) or, alternatively, the nuclear scattering amplitude b for neutrons. The *relative* visibility of the iron and the tantalum in an *equiatomic* parent sample is approximated by the ratio

$$R = \left(f(Q)_{Ta}/f(Q)_{Fe}\right)^2 \approx \left(Z_{Ta}/Z_{Fe}\right)^2$$
$$R = (73/26)^2 = 7.88/1$$

in favour of tantalum, with x-rays. The corresponding ratio for neutrons is,

$$R = \left(b_{Fe}/b_{Ta}\right)^2 \approx (0.95/0.69)^2$$
$$R = 1.89/1$$

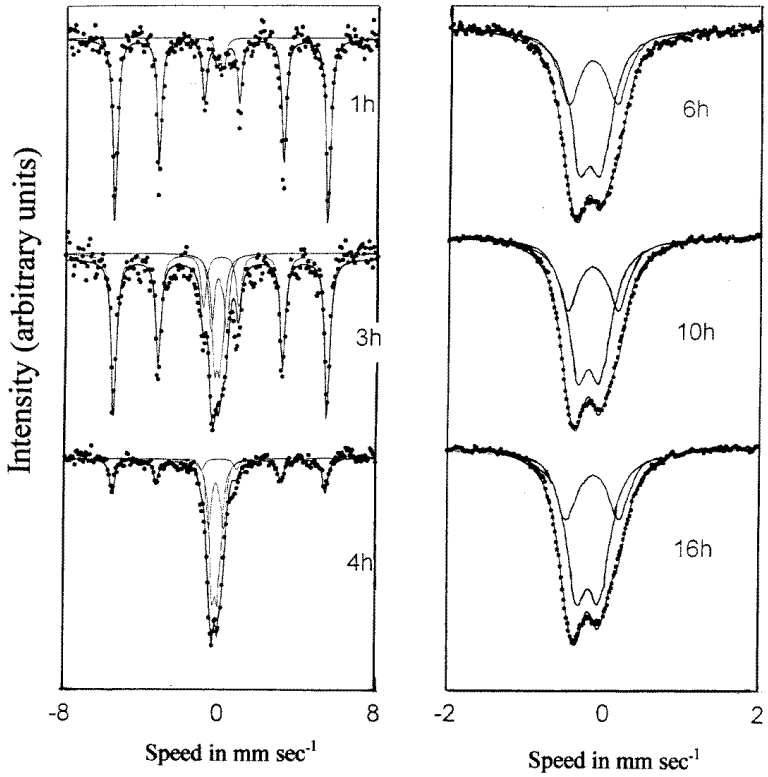

Figure 3. The ^{57}Co Mössbauer spectra measured at 77 K for the $Fe_{58}Ta_{42}$ alloys MA treated for 1, 3, 4, 6, 10 and 16 h. Note that the latter three spectra are plotted over a smaller range of source velocity.

in favour of iron. The neutron diffraction patterns for a series of the $Fe_{58}Ta_{42}$ samples are shown in figure 2. Figures 1 and 2 show that the Bragg peaks from the parent phases broaden and decrease in intensity as the time of MA treatment increases and this can be followed easily for MA times of up to 4 h. A broad, diffuse intensity distribution emerges for longer times of MA treatment and this is indicative of the growing amorphous alloy phase. It is interesting to note that the small (110) peak in the diffraction patterns of the samples MA treated for 6 and 8 h shows that it is the iron which is consumed last in this reaction. The diffraction pattern for the 24 h treated specimens in figure 2 is, in fact, quite characteristic of the *metallic glass* state. The derivation of the structure factor $S(Q)$ and the reduced radial distribution function $G(r)$ of this amorphous alloy has been given in full elsewhere [9].

Examples of the transmission Mössbauer spectra measured at 77 K for the $Fe_{58}Ta_{42}$ samples are shown in figure 3. At least two components can be identified in these spectra, a magnetic sextet and a quadrupolar doublet. The spectra show that as the time of MA treatment increases, the magnetic sextet disappears progressively in favour of the quadrupolar doublet and this indicates that the parent α-Fe is being consumed to form an Fe–Ta alloy phase.

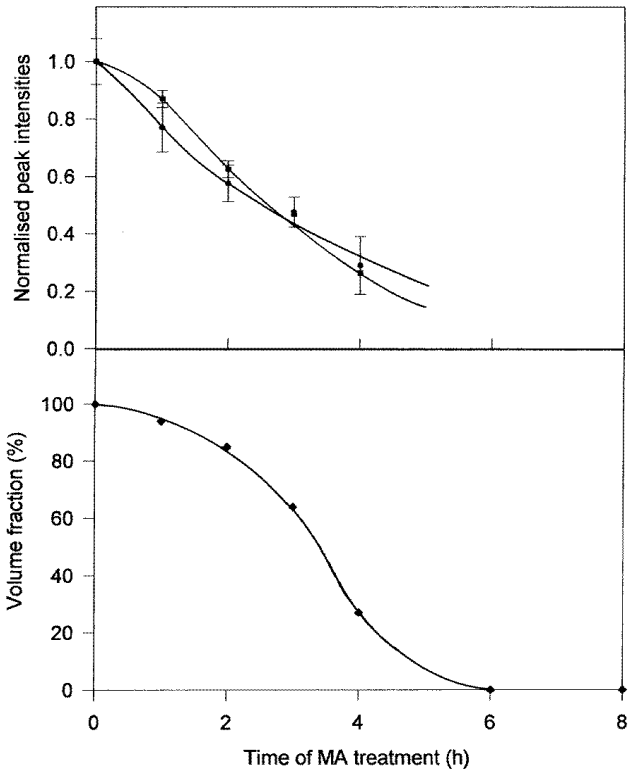

Figure 4. The consumption of the phases in the MA treated $Fe_{58}Ta_{42}$ alloys: top, the consumption of the parent phases from the diffraction data (■, tantalum; ●, iron); bottom, the consumption of the α-Fe fraction from the Mössbauer data.

3. Data analysis

3.1. Neutron and x-ray diffraction

The intensity of each Bragg peak in a diffraction pattern was fitted with a pseudo-Voigt function (see e.g. [10]) and the intensities obtained were summed (ΣI) to the same value of Q for each phase. The intensities were normalized to the sample weight and to the diffraction pattern of the parent alloy, to allow a proper comparison to be made. The results from the neutron diffraction patterns are shown in figure 4. In the early stages of the reaction, the iron appears to be consumed at a faster rate than the tantalum but this is reversed after 3 h MA treatment. Similar data were obtained from the x-ray diffraction patterns although the need for corrections for absorption and self-shielding may be greater in this case. For example, the linear absorption coefficient for an equiatomic FeTa sample is $\mu_x = 938$ cm^{-1} for x-rays and only $\mu_x = 0.41$ cm^{-1} for neutrons. This means that a neutron beam passing through 3 cm of an FeTa sample and an x-ray beam passing through only 14 μm are attenuated by a similar amount ($I/I_0 \approx 30\%$).

The summed Bragg peak intensities (ΣI) shown in figure 4 (top) appear to fall exponentially with time of MA treatment, so the consumption of the parent materials in

the reaction can be described by an equation of the form used by us in the past [11],

$$\Sigma I(t) = \Sigma I(0)\ \exp(-t/\tau)$$

where τ is the time constant of the consumption. For the x-ray data of figure 1, a graph of $\ln(\Sigma I(t)/\Sigma I(0))$ against t for the Bragg peaks from tantalum gave a good straight line whose slope gave $\tau_{Ta} = 3.0$ h, but the less intense Bragg peaks of the α-Fe allowed only an estimate $\tau_{Fe} \approx 2.6$ h to be made. Analysis of the neutron data of figures 2 and 4 gave a good straight line in $\ln(\Sigma I(t)/\Sigma I(0))$ against t for iron and a reliable value $\tau_{Fe} = 4.0$ h. A value $\tau_{Ta} = 3.0$ h was obtained for tantalum corresponding to times of MA treatment greater than 3 h and this is similar to the τ_{Ta} value from the x-ray data. Note that the speed of reaction in this eutectic $Fe_{58}Ta_{42}$ alloy is very much greater than that in $Fe_{80}Ta_{20}$ alloys MA treated in a similar Spex 8000 mill at room temperature and 473 K [6].

3.2. Mössbauer spectrometry

The Mössbauer spectra were analysed using a conventional least-squares refinement method to obtain the best fit to the spectrum from a combination of sextet and doublet signals, whose Mössbauer parameters were given as input data. The fitted spectra and their components are shown in figure 3, which allows the evolution of the phases in the reaction to be followed. The Mössbauer spectra for samples MA treated for *less* than 6 h consist of a magnetic sextet superimposed on an asymmetric quadrupolar doublet. These can be unambiguously attributed to the parent α-iron phase and the emerging Fe–Ta alloy phase respectively. The relative amount of the iron sites and the phases associated with them are proportional to the relative area under the peaks of each component of the Mössbauer spectrum. Thus if the α-Fe and the Fe–Ta alloy phases both have the same value of recoil-free fraction (f-factor), then the relative amount of α-Fe can be determined as a function of time of MA treatment as shown in figure 4 (bottom). This curve is much rounder in outline than those in figure 4 (top).

A more detailed analysis of the Mössbauer spectra has revealed that when the time of MA treatment increases, the spectral lines become slightly broadened. This can be accounted for by using a distribution of hyperfine fields for those samples MA treated for less than 6 h. The hyperfine field distributions obtained consist of a narrow peak centred around 33.9 T, which corresponds to the usual value for b.c.c. α-Fe at 77 K. Thus for these short times of MA treatment most of the iron nuclei which are in a magnetic environment must belong to the b.c.c. α-Fe phase. These hyperfine field distributions do not provide any direct evidence of interface regions between the elemental constituents in this particular solid state reaction.

The Mössbauer spectra for the specimens MA treated for *more* than 6 h exhibit a single *asymmetric* paramagnetic doublet which is consistent with those observed previously in the Mössbauer spectra of MA amorphous Fe_xTa_{1-x} alloys [6] and of amorphous Fe_xTa_{1-x} alloys produced by sputtering [4]. The asymmetry of this doublet is best represented by fitting it with *two* quadrupolar doublets, rather than broad and non-Lorentzian lineshapes, which might be expected for a structurally disordered material. However, it is worth noting that two of the most successful structural models for metallic glasses based on relaxed hard-sphere assemblies [12, 13] both predict that 90% of the local environments can be described in terms of just *two* polyhedra, namely distorted tetrahedra and distorted octahedra.

The values of the hyperfine parameters, i.e. the linewidth at half height ($\Gamma/2$), the quadrupolar splitting (Q.S.), the quadrupolar shift (2ε) and the mean hyperfine field $\langle H_f \rangle$, for all of the components of the Mössbauer spectra are listed in table 1. The values of

Table 1. The values of hyperfine parameters for the components in the Mössbauer spectra, recorded at liquid nitrogen temperature (77 K), of the MA treated $Fe_{58}Ta_{42}$ alloys. The isomer shift (I.S.) values are given relative to α-Fe at 300 K, $\Gamma/2$ is the linewidth at half height, Q.S. is the quadrupolar splitting, 2ε is the quadrupolar shift and $\langle H_f \rangle$ is the hyperfine field.

Time of MA (h)	Component of spectra	I.S. (mm s^{-1})	$\Gamma/2$ (mm s^{-1})	2ε/Q.S. (mm s^{-1})	$\langle H_f \rangle$ (T)	%
1	magnetic sextet	0.10	0.13	0.00	33.8	94.6
	quadrupolar doublet 1	0.01	0.13	0.28	0.0	5.4
2	magnetic sextet	0.11	0.13	0.01	33.9	85
	quadrupolar doublet 1	−0.02	0.16	0.28	0.0	9
	quadrupolar doublet 2	−0.02	0.16	0.78	0.0	6
3	magnetic sextet	0.11	0.15	0.01	33.8	64.0
	quadrupolar doublet 1	−0.05	0.16	0.27	0.0	20.4
	quadrupolar doublet 2	−0.00	0.16	0.71	0.0	15.6
4	magnetic sextet	0.09	0.16	0.00	33.8	27.7
	quadrupolar doublet 1	−0.07	0.16	0.27	0.0	45.4
	quadrupolar doublet 2	−0.05	0.16	0.69	0.0	26.9
6	quadrupolar doublet 1	−0.07	0.16	0.27	0.0	62
	quadrupolar doublet 2	−0.04	0.16	0.61	0.0	38
8	quadrupolar doublet 1	−0.06	0.16	0.28	0.0	63.6
	quadrupolar doublet 2	−0.01	0.16	0.66	0.0	36.4
10	quadrupolar doublet 1	−0.07	0.16	0.28	0.0	62.8
	quadrupolar doublet 2	−0.02	0.16	0.62	0.0	37.1
16	quadrupolar doublet 1	−0.06	0.16	0.28	0.0	64.8
	quadrupolar doublet 2	−0.01	0.16	0.66	0.0	35.2

the hyperfine parameters, for *one* of these components (doublet 1 in the table) are not very different from those of the crystalline intermetallic compound Fe_2Ta measured at 77 K, e.g. I.S. $= -0.13$ mm s^{-1}, $\Gamma/2 = 0.13$ mm s^{-1} and Q.S. $= 0.30$ mm s^{-1}. However, the (negative) values of the isomer shifts for both of the paramagnetic doublets (1 and 2) are larger than the value for the crystalline Fe_2Ta phase. The value of the isomer shift relates to the s-electron density at the ^{57}Fe nuclei and these values for the paramagnetic phases suggest a decrease in the electron density, which is consistent with an increase in the volume associated with the iron atoms. This may be attributed to either an increase of the average Fe–Ta distance, consistent with a greater free volume in the fully transformed FeTa phase, or, alternatively, a difference in the local structural environment, which might be b.c.c. or f.c.c.-like in the MA FeTa phase and is h.c.p. in Fe_2Ta [14, 15]. One may note that a similar dependence of I.S. on particle size has been observed in $BaTiO_3$ perovskites [16].

4. Conclusions

The x-ray and neutron diffraction measurements and Mössbauer spectrometry of MA treated $Fe_{58}Ta_{42}$ alloys are in good agreement and have shown that the solid state reaction is extremely rapid. The parent elements are consumed after just 6 h treatment in a conventional Spex 8000 mill. Three other conclusions arise from the present study.

The Mössbauer measurements do not give any clear evidence for the presence of an intermediate phase or interfacial zones in the reaction. The presence of these zones in MA treated $Fe_{58}Ta_{42}$ (M = Si, V, W, Sn) alloys has been suggested by an analysis of the characteristic hyperfine field distributions observed in Mössbauer spectrometry [7] and also from T.E.M. measurements on $Ni_{50}Zr_{50}$ alloys [17]. In addition, it is clear that neither of

the two components of the asymmetric doublet in the Mössbauer spectra of the samples mechanically alloyed for more than 6 h can be associated with interfacial zones. First, the same kind of asymmetric doublet is seen in the Mössbauer spectra of sputtered Fe_xTa_{1-x} alloys [4], which do not have interfaces of the kind which exist in MA samples. Second, our high-resolution study of the structure of fully transformed $Fe_{58}Ta_{42}$ alloy (MA 24 h) made by pulsed neutron scattering shows unequivocally that this sample is completely amorphous [9]. It is possible, therefore, that the absence of intermediate phases or interfacial zones is connected with the high speed of the reaction in these Fe–Ta alloys.

The diffraction data of figure 4 (top) and the Mössbauer data of figure 4 (bottom) provide slightly different views of the consumption of the constituents in the reaction. The diffraction measurements represent an average over the whole sample and are not particularly sensitive to the presence of *small* volume elements. These are found in the fine lamellar composites which characterize the early stages of MA treatment [11, 18]. It is possible that as the lamellae become finer and more dispersed they are less easily detected by the diffraction measurements. On the other hand, the Mössbauer spectrometry is a site specific technique, so that, providing the iron atoms retain their immediate neighbour environment, the signal from *all* of the iron atoms will be recorded and this is independent of whether they are situated within a fine lamellae or in the bulk of a powder grain. This explanation is consistent with the fact that the main differences between the top and bottom parts of figure 4 correspond to short times of MA treatment 1 h $< t <$ 3 h, when the lamella composites are known to be most strongly developed [11, 18].

The narrow line widths obtained from the Mössbauer data on the samples MA treated for more than 6 h, the presence of just two paramagnetic doublets and the similarities between their hyperfine parameters and those of the Fe_2Ta intermetallic compound obviously raise questions about the structural identity of the fully transformed samples. However, recent differential thermal analysis (DTA) measurements on these $Fe_{58}Ta_{42}$ specimens [19] have provided clear evidence of a crystallization peak, confirming their amorphous state. This is also supported by our analysis of the structural data on the 24 h MA sample referred to above [9]. We believe that these two observations exclude the possibility that the end-product of the reaction is micro-crystalline.

The neutron experiments have been made within the EPSRC Neutron Beam Programme and the help of the staff at ISIS source is gratefully acknowledged. RJC has held an EPSRC studentship during the course of this work and NC would like to acknowledge the hospitality of the Faculté des Sciences, Université du Maine.

References

[1] Geissen B C, Madhava M, Polk D E and Vander Sande J 1976 *Mater. Sci. Eng.* **23** 145–50
[2] Wang R, Mertz M D, Brimhall J L and Dahlgren S D 1978 *Proc. 3rd Int. Conf. on Rapidly Quen. Met.* vol 1 (London: Metals Society) pp 420–3
[3] Davis S, Fischer M, Geissen B C and Polk D E 1978 *Proc. 3rd Int. Conf. on Rapidly Quen. Met.* vol 1 (London: Metals Society) pp 425–305
[4] Chien C L, Liou S H, Ha B K and Unruh K M 1985 *J. Appl. Phys.* **57** 3539–41
[5] Yang E, Wagner C N J and Boldrick M S 1993 *Key Eng. Mater.* **81–83** 63–8
[6] Herr U, Friedrich J and Samwer K 1995 *Nanostruct. Mater.* **6** 707–10
[7] Le Caër G and Delcroix P 1996 *Nanostruct. Mater.* **7** 127–35
[8] Cooper R J 1996 *PhD Thesis* University of Sheffield
[9] Cooper R, Randrianantroandro N, Cowlam N and Greneche J-M *Proc. 9th Int. Conf. on Rapidly Quen. Met. (Bratislava, 1996)* at press
[10] Enzo S, Benedetti A, Fagherazzi G and Polizzi S 1988 *J. Appl. Crystallogr.* **21** 536

[11] Li Meiya, Enzo S, Soletta I, Cowlam N and Cocco G 1993 *J. Phys.: Condens. Matter* **5** 5235
[12] Finney J L and Wallace J 1981 *J. Non-Cryst. Solids* **43** 165–87
[13] Lançon F, Billard L and Chamberod A 1984 *J. Phys. F: Met. Phys.* **14** 579–91
[14] Nevitt M N, Kimball C W and Preston R S 1964 *ICM Proc. (Nottingham)* p 137
[15] Pipkorn D N, Edge C K, Debrunner P, de Pasquali G, Drickamer H G and Frauenfelder H 1964 *Phys. Rev.* A **1604** 135
[16] Perriat P and Niepce J C 1994 *High Temp. Chem. Process* **3** 585–600
[17] Shultz L and Eckert J 1995 *Applied Physics* ed H Beck and H J Güntherodt (Berlin: Springer) pp 72, 79–8
[18] Cocco G, Cowlam N and Enzo S 1994 *Mater. Sci. Eng.* A **178** 29
[19] Randrianantroandro N, Cooper R, Greneche J-M and Cowlam N to be published